AGU PUBLICATIONS

Geophysical Research Letters

RESEARCH LETTER
10.1002/2013GL058705

Key Points:
- The observed weakening of EASM is reproduced in CMIP5 models
- The aerosol weakens the monsoon by reducing the land-sea thermal contrast
- The aerosol plays a primary role in driving models' monsoon weakening

Supporting Information:
- Readme

Correspondence to:
T. Zhou,
Zhoutj@lasg.iap.ac.cn

Citation:
Song, F., T. Zhou, and Y. Qian (2014), Responses of East Asian summer monsoon to natural and anthropogenic forcings in the 17 latest CMIP5 models, *Geophys. Res. Lett.*, *41*, doi:10.1002/2013GL058705.

Received 14 NOV 2013
Accepted 20 DEC 2013
Accepted article online 23 DEC 2013

Responses of East Asian summer monsoon to natural and anthropogenic forcings in the 17 latest CMIP5 models

Fengfei Song[1,2], Tianjun Zhou[1,3], and Yun Qian[4]

[1]State Key Laboratory of Numerical Modeling for Atmospheric Sciences and Geophysical Fluid Dynamics, Institute of Atmospheric Physics, Chinese Academy of Sciences, Beijing, China, [2]University of Chinese Academy of Sciences, Beijing, China, [3]Climate Change Research Center, Chinese Academy of Sciences, Beijing, China, [4]Atmospheric Sciences and Global Change Division, Pacific Northwest National Laboratory, Richland, Washington, USA

Abstract In this study, we examined the responses of East Asian summer monsoon (EASM) to natural (solar variability and volcanic aerosols) and anthropogenic (greenhouse gasses and aerosols) forcings simulated in the 17 latest Coupled Model Intercomparison Program phase 5 models with 105 realizations. The observed weakening trend of low-level EASM circulation during 1958–2001 is partly reproduced under all-forcing runs. A comparison of separate forcing experiments reveals that the aerosol forcing plays a primary role in driving the weakened low-level monsoon circulation. The preferential cooling over continental East Asia caused by aerosol affects the monsoon circulation through reducing the land-sea thermal contrast and results in higher sea level pressure over northern China. In the upper level, both natural forcing and aerosol forcing contribute to the observed southward shift of East Asian subtropical jet through changing the meridional temperature gradient.

1. Introduction

The East Asian summer monsoon (EASM) is the most important climate system over East Asia, which provides about 40 ~ 50% (60 ~ 70%) of the annual mean precipitation over southern China (northern China) [*Lei et al*., 2011]. However, during the second half of the twentieth century, the EASM circulation has undergone a weakening tendency, which is featured by a decreasing low-level southwesterly wind, southward shift of East Asian subtropical jet (EASJ) and an increase of sea level pressure (SLP) over East Asia [*Wang*, 2001; *Guo et al*., 2003; *Yu et al*., 2004; *Yu and Zhou*, 2007]. Associated with the weakening of EASM circulation, precipitation increases along the middle and lower reaches of Yangtze River valley and decreases over northern China, exhibiting a so-called "southern-flood-northern-drought" (SFND) pattern [*Gong and Ho*, 2002].

The mechanism responsible for the decadal weakening of EASM is an active research topic. The possible reasons include natural factors (solar variability, volcanic eruptions, and internal variability) and anthropogenic factors (greenhouse gas (GHG) and anthropogenic aerosols). The Pacific Decadal Oscillation (PDO), as an internal variability mode of climate system, is regarded as one of forcing mechanisms [*Yang and Lau*, 2004; *Li et al*., 2010b]. Some studies also suggest that the weakening of EASM may be a response to global warming driven by the increased GHG [*Ueda et al*., 2006; *Zhu et al*., 2012]. In addition, the increased air pollution is also suggested as one of the mechanisms responsible for the weakening of EASM [*Menon et al*., 2002; *Qian et al*., 2003, 2009; *He et al*., 2013; *Wang et al*., 2013]. Recently, *Lei et al*. [2014] suggested that both internal variability and anthropogenic forcing play roles in the observed weakening of EASM. Up to now, there is no consensus on the mechanisms of EASM weakening [*Zhou et al*., 2009].

In the results of coupled model simulation from the ongoing Coupled Model Intercomparison Program phase 5 (CMIP5), since the observed temporal phases of internal variability modes such as El Nino Southern Oscillation and PDO can not be reproduced by specifying external forcings, the natural forcing only refers to solar and volcanic factors. In this study, we examine responses of EASM to natural and anthropogenic forcings simulated by 17 latest CMIP5 models (see Table S1 of the supporting information for the model details), which are driven respectively by GHG, natural forcings, and a combination of all forcings. We aim to understand the following questions: (1) Can the observed weakening tendency of EASM circulation be reproduced in 17 CMIP5 models by specifying the external forcings? (2) If they can, what are relative contributions of different external forcings to the decadal weakening of EASM circulation? (3) How does the external forcing result in the change of EASM circulation?

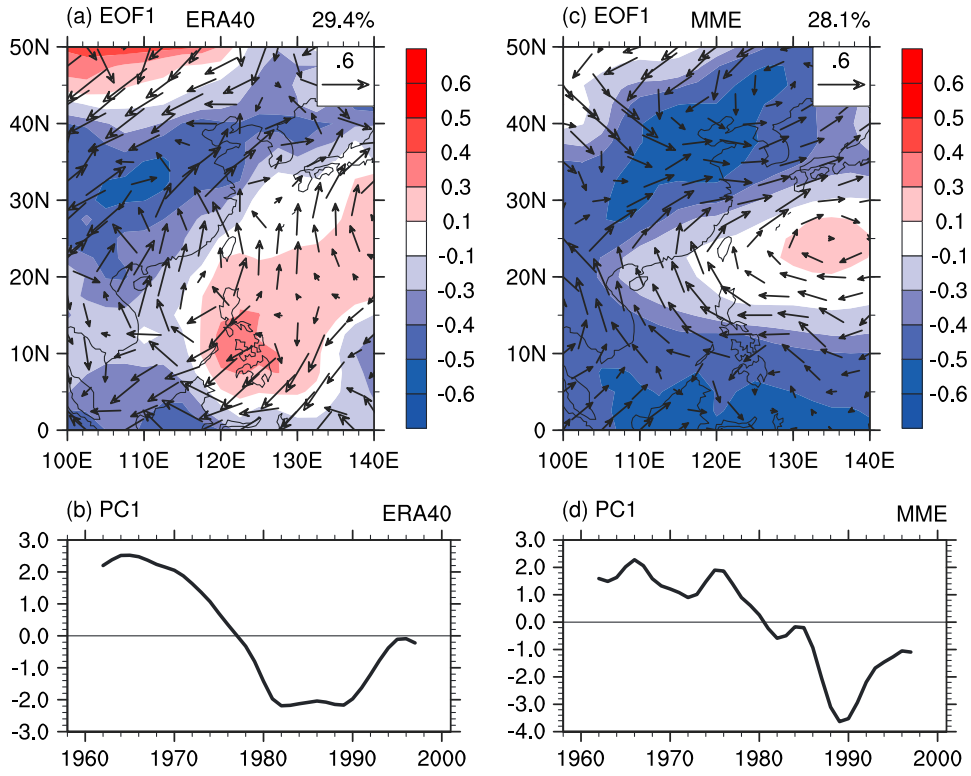

Figure 1. (top) The leading MV-EOF patterns and corresponding PC of SLP (shaded) and 850 hPa winds (vectors) in (left) ERA-40 and (right) MME. The percentage at the right corner is explained variance. The MME is constructed by using 35 realizations from 17 CMIP5 models (see supporting information for details).

2. Model Experiments, Observations, and Method

We analyze the total 105 simulations from 17 CMIP5 models which include 35 historical, historical GHG, and historical natural experiments (see Table S2 of the supporting information), respectively. The historical simulations (named as all forcing) are forced by both natural (solar variability and volcanic aerosols) and anthropogenic forcings (GHG and anthropogenic aerosols) (see Table S3 of the supporting information). The historical GHG (named as GHG forcing) and historical natural (named as natural forcing) simulations are the same as the historical simulations except that they are forced by well-mixed GHG changes or natural variations only. In the analysis, following *Taylor et al.* [2009], the response to anthropogenic forcing is calculated as the difference between all-forcing and natural-forcing runs. The response of aerosol forcing is calculated as the difference between anthropogenic-forcing and GHG-forcing runs.

The following observational and reanalysis data sets are used: (1) monthly mean SLP and 850 hPa winds from European Centre for Medium-Range Weather Forecasts 40-year Re-Analysis (ERA-40) [*Uppala et al.*, 2005] and (2) monthly mean surface air temperature (SAT) anomalies from Goddard Institute for Space Studies Surface Temperature Analysis (GISTEMP) [*Hansen et al.*, 2010].

All the model outputs are interpolated into common 2.5° × 2.5° grid by bilinear interpolation. We focus on the linear trends in the boreal summer (June-July-August mean, JJA) during 1958–2001. To determine the leading mode of EASM decadal variability, the multivariate empirical orthogonal function (MV-EOF) on the three atmospheric circulation fields (SLP, meridional and zonal wind at 850 hPa) is performed over the EASM region (0°N–50°N, 100°E–140°E), following the observational analysis method of *Wang et al.* [2008]. Before the MV-EOF, the 7 year low-pass filter is applied to suppress the interannual variability.

3. Results

The leading MV-EOF mode in the observation and the all-forcing run of multimodel ensemble mean (MME) are shown in Figure 1. The leading mode in the observation accounts for 29.4% of the total variance for all

three fields together (Figure 1a). The spatial pattern of the leading mode shows low pressure extending from the southwestern China to South Korea/North Korea and high pressure over the northwestern Pacific (NWP). At 850 hPa, an anticyclone is evident over the NWP, and southerly winds dominate eastern China. The principal component of the leading mode (PC1) exhibits a decreasing trend, indicative of the weakening tendency of EASM circulation (Figure 1b). The PC1 has been stable since the 1980s and tends to recover from the 1990s, indicating the recovery of EASM circulation as noted in previous studies [*Liu et al*., 2012]. Compared to the observation, the anticyclone in the MME shifts northward and appears well organized (Figure 1c). The pattern correlation of SLP between the MME and observation is 0.68, which is statistically significant at the 5% level. The PC1 in the MME also exhibits a declining trend and has recovered since the 1990s (Figure 1d). A further MV-EOF analysis on the different forcing runs shows that aerosol forcing contributes most to the EASM weakening, while the GHG forcing favors an enhanced monsoon circulation (Figure S1 of the supporting information). The correlation coefficient for the PC1 in the observation and MME is 0.78, which is statistically significant at the 1% level. Hence, the observed leading mode has been well captured by the MME in the context of both spatial pattern and temporal evolution.

The different forcing runs from the MME are analyzed to investigate their contributions to the declining trend of EASM. The linear trends of SLP and 850 hPa winds during 1958–2001 in the observation and different runs of MME are shown in Figure 2. The positive trends of SLP over northern China and negative trends of SLP over the NWP are seen in both the observation and all-forcing run (Figures 2a and 2b). To be consistent with 850 hPa winds, SLP in the observation is also from ERA-40 but HadSLP2 [*Allan and Ansell*, 2006] shows similar results (Figure S2 of the supporting information). The cyclone circulation over the NWP and northerly winds over eastern China are also evident. The similarity between the leading mode and the trend pattern suggests that the leading mode reflects the trend of EASM circulation. The anthropogenic-forcing run displays a similar pattern as the all-forcing run, indicating a dominant role of anthropogenic-forcing agents (Figure 2c). In contrast, the anticyclone and southerly winds dominate eastern China in the GHG-forcing runs (Figure 2d). The SLP and wind response to the natural forcing is weak (Figure 2e). The response of SLP in the aerosol-forcing run features a meridional dipole pattern, with positive anomalies over northern China and negative anomalies over southern China (Figure 2f). Correspondingly, eastern China is dominated by northerly wind anomalies, indicating a weakened summer monsoon circulation.

To understand the physical processes through which external forcings alter the monsoon circulation patterns, the linear trends of SAT in the observation and MME are displayed in Figure 3. Over eastern China, the surface cooling is evident in the observation (see the box of Figure 3a). In the all-forcing run, the magnitude of cooling in the region is weaker, but the pattern is similar to the observation (Figure 3b). In the GHG-forcing run, the magnitude of the warming over the land is larger than that over the ocean (Figure 3d) because the heat capacity of the latter is larger. Due to the same reason, the magnitude of cooling over the land is larger than that over the ocean in the aerosol-forcing run (Figure 3f). Besides this, the anthropogenic aerosol loading over East Asia is larger than elsewhere [*Menon et al*., 2002; *Wang et al*., 2013], so the surface cooling over East Asian continent is the strongest (Figure 3f). Since the aerosol-induced cooling is offset by the GHG-induced warming, a weak cooling trend is displayed over eastern China in the anthropogenic-forcing run (Figure 3c). The natural forcing mainly cools southern China (Figure 3e).

A comparison of Figure 2 with Figure 3 shows that the surface cooling over central China may induce the positive SLP trends over northern China. To demonstrate this hypothesis, the scatterplot between SLP and SAT trends in 17 models is shown in Figure 4a. An inverse relationship between SAT and SLP trends is evident in all simulations. This is also supported by the fitting coefficients, which are all statistically significant at the 5% level based on the Student's *t* test except for GHG-forcing runs. Hence, the surface cooling over eastern China weakens the land-sea thermal contrast and further induces the positive SLP trends over northern China.

The weakening trend of EASM circulation is driven by the decreased land-sea thermal contrast. This is evidenced by the linear trends of SAT over central China (Figure 4b). In the observation, central China has undergone a significant cooling trend (-0.70 K (44 year)$^{-1}$) during 1958–2001. The cooling trend over central China will reduce the land-sea thermal contrast. Under all-forcing runs, the cooling trend is captured except with a smaller magnitude (-0.18 K (44 year)$^{-1}$), but it is still statistically significant at the 5% level. Anthropogenic forcing contributes 83.8% to the all forcing cooling following the linearity assumption [*Taylor et al*., 2009]. The warming trend over central China is evident in the GHG-forcing run due to the smaller heat

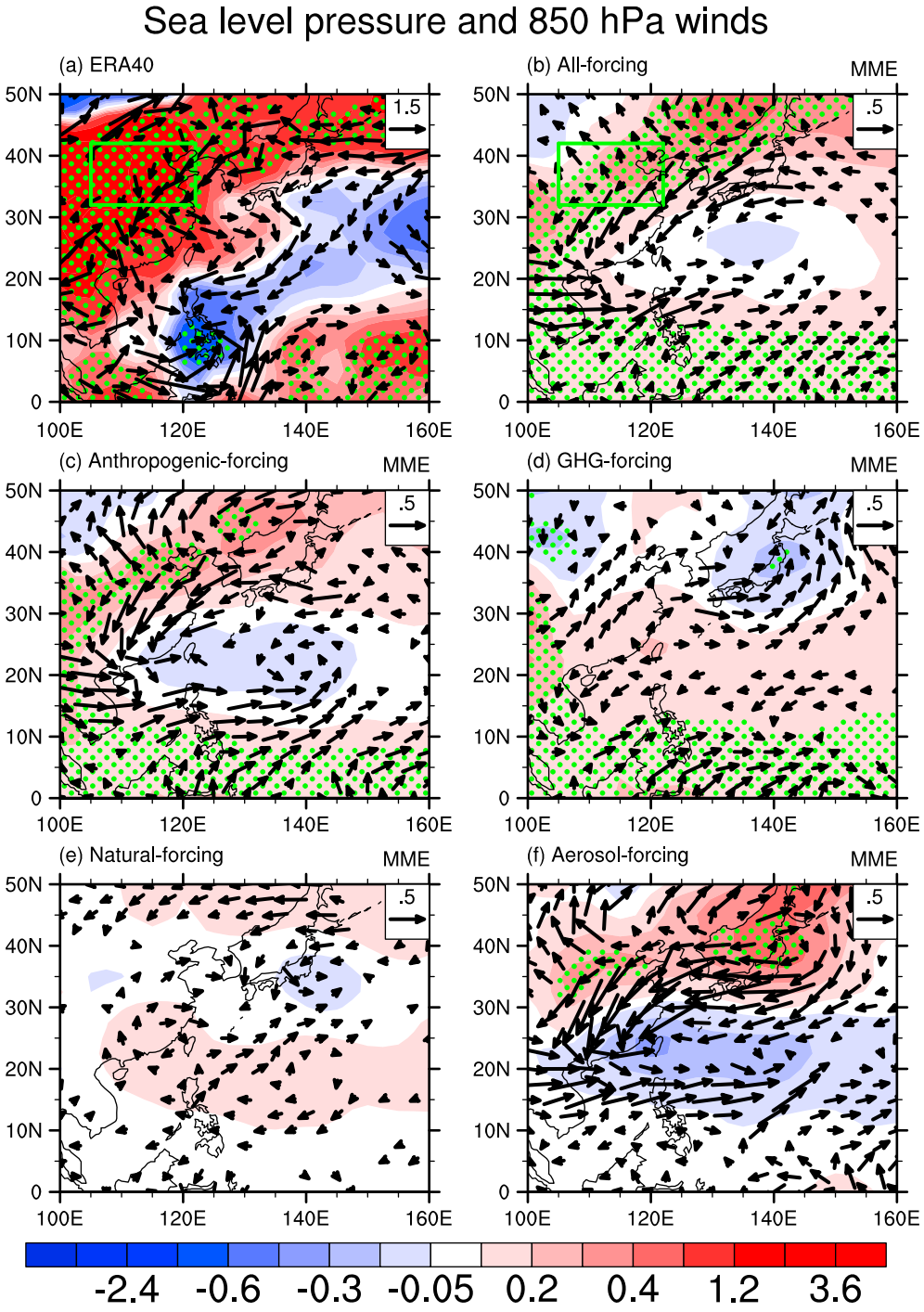

Figure 2. The linear trends of SLP (shaded; hPa $(44\,\text{year})^{-1}$) and 850 hPa winds (vectors; m s^{-1} $(44\,\text{year})^{-1}$) in JJA during 1958–2001. (a) Observations (SLP and 850 hPa winds from ERA-40), (b) all-forcing run, (c) anthropogenic-forcing run, (d) GHG-forcing run, (e) natural-forcing run, and (f) aerosol-forcing run from MME. The green box in Figures 2a and 2b is northern China (32°N–42°N, 105°E–122°E). The dotted areas indicate that the precipitation trends are statistically significant at the 10% level. The MME is constructed by using 35 realizations from 17 CMIP5 models (see supporting information for details).

capacity over land, while the cooling trend is more significant in the aerosol-forcing run due to the preferential cooling over East Asia. Hence, the aerosol forcing plays a primary role in the central China cooling and weakened land-sea thermal contrast. In addition, the surface cooling and rainfall decrease may form a positive feedback as suggested by *Li et al.* [2010a].

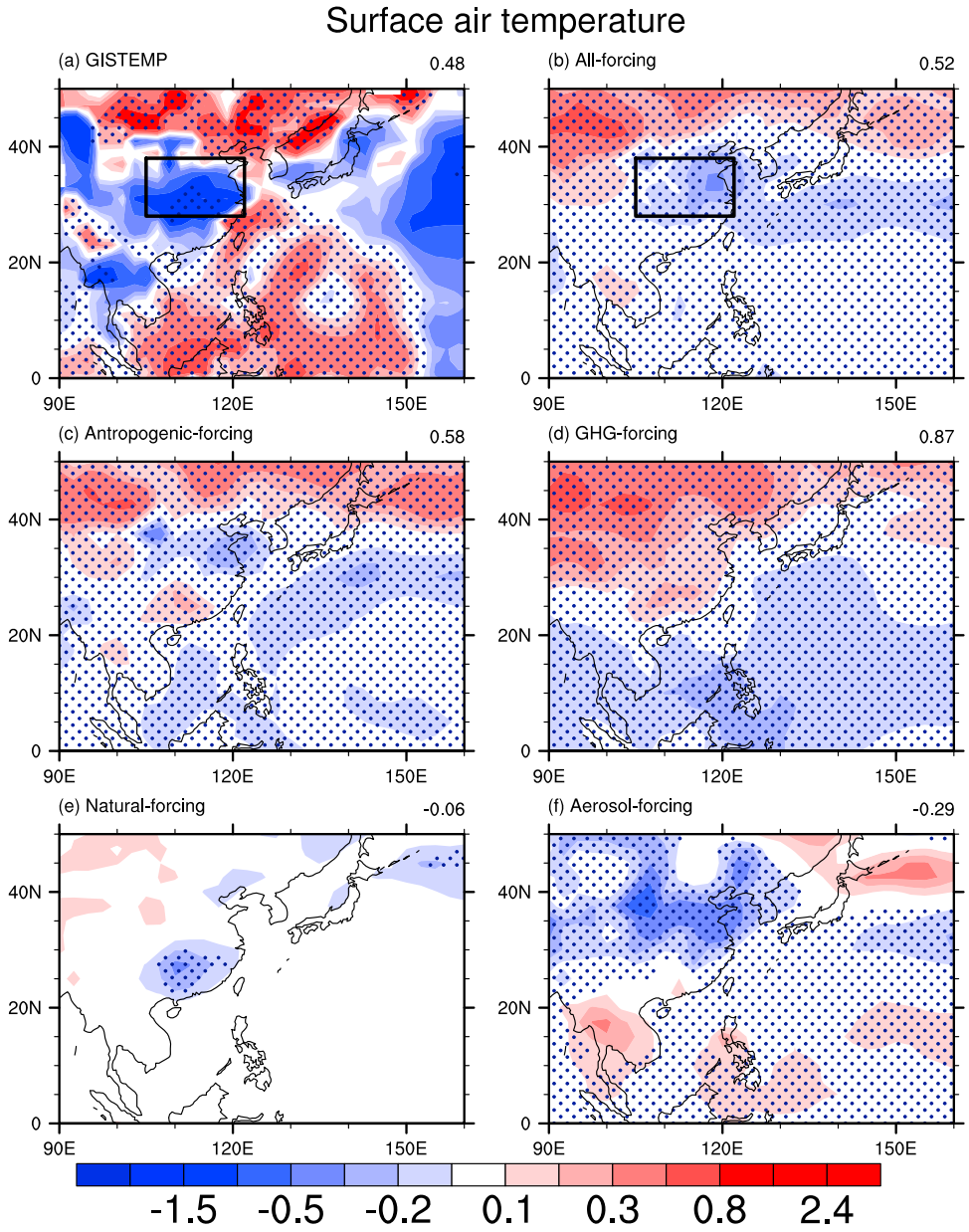

Figure 3. Same as Figure 2 but for SAT trends (K (44 year)$^{-1}$). (a) The observation is from GISTEMP. (a and b) The black boxes are eastern China (28°N–38°N, 105°E–122°E). The domain average has been subtracted and shown in the right corner. The MME is constructed by using 35 realizations from 17 CMIP5 models (see supporting information for details).

The EASJ is an important component of EASM and can induce uplift over and bring transient eddies to eastern China, anchoring the EASM rainband [*Sampe and Xie*, 2010]. The linear trends of EASJ during 1958–2001 under different forcing runs are shown in Figure S3 of the supporting information. The observed southward shift of EASJ [*Yu et al.*, 2004] can be partly reproduced in the all-forcing run, although with weaker magnitude (Figures S3a and S3b of the supporting information). The natural forcing (aerosol forcing) contributes to the southward shift of its eastern (western) part (Figures S3e and S3f of the supporting information). In the GHG-forcing run, the EASJ is intensified but not shifted southward (Figure S3d of the supporting information). Further analyses show that the changes of EASJ under different separate forcings are consistent with the changes of meridional temperature gradient (MTG) (Figure S4 of the supporting information).

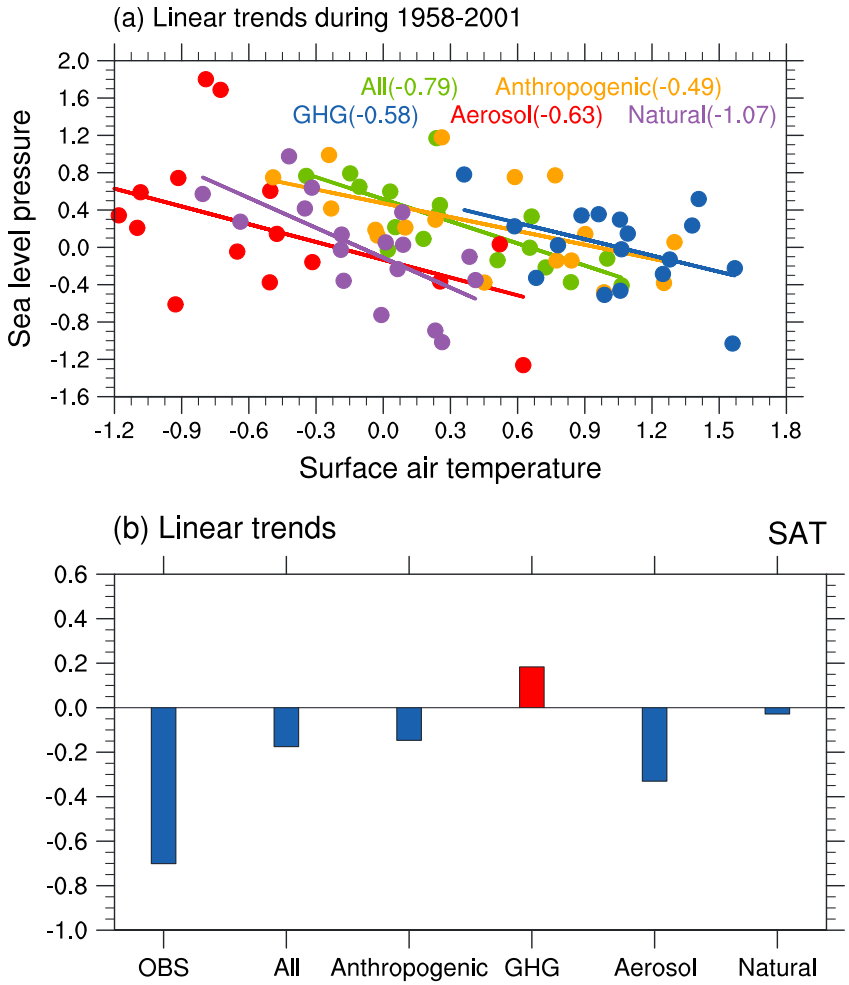

Figure 4. (a) Scatterplot of the linear trends of SAT (K (44 year)$^{-1}$) averaged over eastern China (28°N–38°N, 105°E–122°E) and SLP (hPa (44 year)$^{-1}$) averaged over northern China (32°N–42°N, 105°E–122°E) in JJA during 1958–2001. The dots indicate 17 models in different forcing runs identified by different colors. The lines indicate the best linear fit lines between SAT and SLP. The fitting coefficients are given in the brackets. (b) Linear trends of SAT averaged over eastern China (28°N–38°N, 105°E–122°E) in the observation, all-forcing run, anthropogenic-forcing run, GHG-forcing run, aerosol-forcing run, and natural-forcing run of MME (the SAT averaged over the EASM region (0°N–50°N, 90°E–160°E) have been subtracted). The MME is constructed by using 35 realizations from 17 CMIP5 models (see supporting information for details).

4. Summary and Discussion

The influence of different forcings on the weakening of EASM circulation during 1958–2001 is examined by analyzing 105 realizations from the 17 latest CMIP5 models. The results show that the weakening of EASM circulation is partly reproduced under all-forcing runs. A comparison of separate forcing runs shows that the aerosol forcing plays a primary role in the weakening of EASM in the all-forcing run. The contribution of natural forcing is nearly negligible. The GHG forcing favors a slightly enhanced rather than weakened monsoon circulation. The land-ocean heat capacity contrast makes the land warm more than the ocean under GHG forcing and the land cool more under aerosol forcing. Besides this, the aerosol forcing also drives a preferential cooling over the emission source regions. The combined effects of GHGs and aerosols (anthropogenic forcing) make East Asia cooler than other neighboring regions. Positive SLP trends over northern China are induced by the weakened land-sea thermal contrast. The low-level divergence is induced by the positive SLP trends and leads to a weakening of EASM circulation. In the upper level, the observed southward shift of EASJ is partly captured in the all-forcing run and contributed by both natural forcing and aerosol forcing through the change of MTG.

Some limitations of the study should be acknowledged. First, the linearity assumption is adopted from the work of *Taylor et al.* [2009] to investigate the roles of different external forcings. However, whether the responses of climate system to different forcings are linear remains to be verified in the future.

Second, the observed weakening trend of EASM circulation at the decadal time scale is driven by both the internal variability and external forcing. Our analysis presented here is based on MME, and thus, the internal variability is removed largely due to the ensemble technique. Through our analysis, we suggest that the external forcing plays a significant role in the decadal weakening of EASM circulation. However, the decreasing trends of EASM under external forcing is weaker than the observation, as evidenced in the circulation trend pattern (Figure 2b), SAT trend magnitude (Figure 4b). This discrepancy indicates that the internal variability mode of PDO may play a dominant role in the monsoon weakening as previously suggested [*Li et al*., 2010b; *Lei et al*., 2014; *Zhou et al*., 2013], while the aerosol forcing plays a secondary or complementary role. Considering the model uncertainty and nonlinearity, how to determine the relative contributions of internal variability and external forcing deserves further study.

Third, although the EASM circulation trend is partly captured in the MME, the SFND pattern is still a challenge for current models (Figure S5 of the supporting information). As discussed by *Li et al*. [2010b], the observed small-scale monsoon rainband cannot be accurately described by relatively lower resolution models, thus the limitation of CMIP5 models in the simulation of SFND pattern is not unexpected. Whether high-resolution models can improve the simulation of monsoon rainband in the context of both climatology and the changes deserves further study.

Finally, we focus on the decline trend of EASM circulation during the last 50 years in this study, but we also notice that the all-forcing run of MME has a considerable ability to reproduce the recovery of EASM since the 1990s. Although the aerosol forcing over East Asia is still increasing after the 1990s, the local surface air temperature change has followed the global aerosol forcing and has not decreased [*Xie et al*., 2013]. This partly explains why EASM has also recovered since 1990s in the aerosol-forcing run (Figure S1 of the supporting information), but the relative contributions of different forcings deserve further study.

Acknowledgments

This work is supported by National Natural Science Foundation of China under grant 41125017. The contribution of Yun Qian in this study is supported by the U.S. Department of Energy's Office of Science as part of the Regional and Global Climate Modeling Program. The Pacific Northwest National Laboratory is operated for DOE by Battelle Memorial Institute under contract DE-AC05-76RL01830.

The Editor thanks two anonymous reviewers for their assistance in evaluating this paper.

References

Allan, R., and T. Ansell (2006), A new globally complete monthly historical gridded mean sea level pressure dataset (HadSLP2): 1850–2004, *J. Clim.*, *19*, 5816–5842.

Gong, D., and C. Ho (2002), Shift in the summer rainfall over the Yangtze River valley in the late 1970s, *Geophys. Res. Lett.*, *29*(10), 1436, doi:10.1029/2001GL014523.

Guo, Q., J. Cai, X. Shao, and W. Sha (2003), Interdecadal variability of East Asian summer monsoon and its impact on the climate of China, *Acta. Geogr. Sin.*, *58*, 569–576 (in Chinese).

Hansen, J., R. Ruedy, M. Sato, and K. Lo (2010), Global surface temperature change, *Rev. Geophys.*, *48*, RG4004, doi:10.1029/2010RG000345.

He, B., Q. Bao, J. Li, G. Wu, Y. Liu, X. Wang, and Z. Sun (2013), Influences of external forcing changes on the summer cooling trend over East Asia, *Clim. Change*, *117*, 829–841.

Lei, Y., B. Hoskins, and J. Slingo (2011), Exploring the interplay between natural decadal variability and anthropogenic climate change in summer rainfall over china. Part I: observational evidence, *J. Clim.*, *24*, 4584–4599.

Lei, Y., B. Hoskins, and J. Slingo (2014), Natural variability of summer rainfall over China in HadCM3, *Clim. Dyn.*, *42*, 417–432.

Li, C., T. Li, J. Liang, D. Gu, A. Lin, and B. Zheng (2010a), Interdecadal variations of meridional winds in the South China Sea and their relationship with summer climate in China, *J. Clim.*, *23*, 825–841.

Li, H., A. Dai, T. Zhou, and J. Lu (2010b), Responses of East Asian summer monsoon to historical SST and atmospheric forcing during 1950–2000, *Clim. Dyn.*, *34*, 501–514, doi:10.1007/s00382-008-0482-7.

Liu, H., T. Zhou, Y. Zhu, and Y. Lin (2012), The strengthening East Asia summer monsoon since the early 1990s, *Chin. Sci. Bull.*, *57*, 1553–1558, doi:10.1007/s11434-012-4991-8.

Menon, S., J. Hansen, L. Nazarenko, and Y. Luo (2002), Climate effects of black carbon aerosols in China and India, *Science*, *297*, 2250–2253.

Qian, Y., L. Leung, S. Ghan, and F. Giorgi (2003), Regional Climate Effects of Aerosols Over China: Modeling and Observation, *Tellus Ser. B Chem. Phys. Meteorol.*, *55*(4), 914–934.

Qian, Y., D. Gong, J. Fan, L. Leung, R. Bennartz, D. Chen, and W. Wang (2009), Heavy pollution suppresses light rain in China: Observations and modeling, *J. Geophys. Res.*, *114*, D00K02, doi:10.1029/2008JD011575.

Sampe, T., and S.-P. Xie (2010), Large-scale dynamics of the Meiyu-Baiu rain band: Environmental forcing by the westerly jet, *J. Clim.*, *23*, 113–134.

Taylor, K. E., R. J. Stouffer, and G. A. Meehl (2009), A summary of the CMIP5 experiment design. PCDMI Rep., 33 pp., [Available online at http://cmip-pcmdi.llnl.gov/cmip5/docs/Taylor_CMIP5_design.pdf].

Ueda, H., A. Iwai, K. Kuwako, and M. E. Hori (2006), Impact of anthropogenic forcing on the Asian summer monsoon as simulated by eight GCMs, *Geophys. Res. Lett.*, *33*, L06703, doi:10.1029/2005GL025336.

Uppala, M., et al. (2005), The ERA-40 reanalysis, *Q. J. R. Meteorol. Soc.*, *131*, 2961–3012.

Wang, B., Z. Wu, J. Li, J. Liu, C. P. Chang, Y. Ding, and G. Wu (2008), How to Measure the Strength of the East Asian Summer Monsoon, *J. Clim.*, *21*, 4449–4463.

Wang, H. (2001), The weakening of Asian monsoon circulation after the end of 1970s, *Adv. Atmos. Sci.*, *18*, 376–386, doi:10.1007/BF02919316.

Wang, T., H. Wang, H. Ottera, Y. Gao, L. Suo, T. Furevik, and L. Yu (2013), Anthropogenic forcing of precipitation pattern in Eastern China in late 1970s, *Atmos. Chem. Phys.*, *13*, 12,433–12,450, doi:10.5194/acp-13-12433-2013.

Xie, S.-P., B. Lu, and B. Xiang (2013), Similar spatial patterns of climate responses to aerosol and greenhouse gas changes, *Nat. Geosci.*, *6*, 828–832.

Yang, F., and K. Lau (2004), Trend and variability of China precipitation in spring and summer: Linkage to sea surface temperatures, *Int. J. Climatol.*, *24*, 1625–1644.

Yu, R., and T. Zhou (2007), Seasonality and three-dimensional structure of interdecadal change in the East Asian monsoon, *J. Clim.*, *20*, 5344–5355.

Yu, R., B. Wang, and T. Zhou (2004), Tropospheric cooling and summer monsoon weakening trend over East Asia, *Geophys. Res. Lett.*, *31*, L22212, doi:10.1029/2004GL021270.

Zhou, T., D. Gong, J. Li, and B. Li (2009), Detecting and understanding the multi-decadal variability of the East Asian Summer Monsoon – Recent progress and state of affairs, *Meteorol. Z.*, *18*(4), 455–467.

Zhou, T., F. Song, R. Lin, X. Chen, and X. Chen (2013), Explaining extreme events of 2012 from a climate perspective, *Bull. Am. Meteorol. Soc.*, *94*, S1–S74, doi:10.1175/BAMS-D-13-00085.1.

Zhu, C., B. Wang, W. Qian, and B. Zhang (2012), Recent weakening of northern East Asian summer monsoon: A possible response to global warming, *Geophys. Res. Lett.*, *39*, L09701, doi:10.1029/2012GL051155.